

# Head-steered channel selection method for hearing aid applications using remote microphones

Vasudha Sathyapriyan   Michael S. Pedersen   Mike Brookes  
Jan Østergaard   Patrick A. Naylor   Jesper Jensen

**Abstract**—We propose a channel selection method for hearing aid applications using remote microphones, in the presence of multiple competing talkers. The proposed channel selection method uses the hearing aid user’s head-steering direction to identify the remote channel originating from the frontal direction of the hearing aid user, which captures the target talker signal. We pose the channel selection task as a multiple hypothesis testing problem, and derive a maximum likelihood solution. Under realistic, simplifying assumptions, the solution selects the remote channel which has the highest weighted squared absolute correlation coefficient with the output of the head-steered hearing aid beamformer. We analyze the performance of the proposed channel selection method using close-talking remote microphones and table microphone arrays. Through simulations using realistic acoustic scenes, we show that the proposed channel selection method consistently outperforms existing methods in accurately finding the remote channel that captures the target talker signal, in the presence of multiple competing talkers, without the use of any additional sensors.

**Index Terms**—Hearing aids, wireless acoustic sensor network, microphone selection.

## I. INTRODUCTION

Microphone arrays are used in various speech and audio signal processing applications, due to their ability to exploit the spatial diversity of the acoustic scene to selectively enhance the signals appearing from a chosen direction [1]. They are typically used in applications such as hearing aids (HAs) [2], wireless acoustic sensor networks (WASNs) [3], automatic speech recognition (ASR) [4], and teleconferencing systems [1].

The performance of microphone arrays depends not only on the number of microphones but also on the signal-to-noise ratio (SNR) and the direct-to-reverberant ratio (DRR) of the target signal captured by them [1]. In particular, when the microphones are positioned far from the target talker, they tend to capture low SNR and low DRR signals, limiting their noise reduction performance. In applications such as HAs, where microphone placement is constrained by the device size, only

the local acoustic field around the user’s head is sampled, thus limiting noise reduction compared to using a remote microphone (RM) positioned closer to the target source [5], [6], [7], [8]. To address this, it has been proposed to employ multiple RMs in WASNs, where microphones are distributed across the acoustic scene, covering a larger physical area [3], [9], [10]. This approach can capture the target signal at a higher SNR and DRR, even in complex, dynamic acoustic environments.

However, using multiple RMs comes with the demand for more power, bandwidth, and computational resources, the availability of which can be limited, especially in small, battery-powered devices such as HAs. In [11], [12], [13], the authors show that in WASNs, using a particular subset of RM channels can achieve essentially the same performance as using all available RM channels in the room. In particular, using the sensor with the microphone channel located closest to the target talker significantly enhances the target talker signal. Methods using utility functions, which measure the cost of adding or removing a remote sensor to the signal estimation task, have been used for remote channel selection (CS) [13], [14], [15], [16], [17], [18], [19], [20], [21], [22]. In [13], [14], [15], [16], [17], the authors used minimum mean-square error (MMSE) utility function for the signal estimation task. However, these methods assume knowledge of inter-channel second-order statistics (SOS) related to the target talker signal, or estimate them under the assumption of a single-talker environment, i.e., when the acoustic scene consists of only the target talker in noise, but with no competing talkers. Furthermore, in [18], [19], [20], [21], [22], the authors proposed network-aware optimal microphone selection methods. Although the work in [18], [19] focused on minimizing communication cost while limiting output noise power, the authors in [20], [21], [22] proposed network-aware microphone selection methods that are not limited to a specific application. However, these methods either assume that the target talker signal is the only coherent signal captured by all the remote channels, or used the knowledge of its location to characterize it as the dominant source in a multi-talker environment, i.e., when the acoustic scene consists of competing talkers in addition to the target talker.

In the context of automatic speech recognition, various remote CS strategies have been proposed based on choosing the RM channel with the highest SNR [23], the RM channel with the highest DRR [24], the RM channels with the maximum cross-correlation with each other [11], or by clustering RM channels according to their proximity to the target talker [25]. However, SNR-based methods are sensitive to the quality of

This project has received funding from the European Union’s Horizon 2020 research and innovation programme under the Marie Skłodowska-Curie grant agreement No. 956369.

Vasudha Sathyapriyan, Michael S. Pedersen and Jesper Jensen are with Demant A/S, 2765 Smørum, Denmark (e-mail: vasy, micp, jesj@demant.com). Vasudha Sathyapriyan and Jesper Jensen are also with the Department of Electronic Systems, Aalborg University, 9220 Aalborg, Denmark

Mike Brookes and Patrick A. Naylor are with the Department of Electrical and Electronic Engineering, Imperial College London, London SW7 2AZ, United Kingdom (e-mail: mike.brookes, p.naylor@imperial.ac.uk).

Jan Østergaard is with the Department of Electronic Systems, Aalborg University, 9220 Aalborg, Denmark (e-mail: jo@es.aau.dk).

the voice activity detectors (VADs) in noisy environments, and a good estimation of the room impulse response (RIR) can be challenging in highly dynamic environments for the DRR-based method. Furthermore, the multi-channel cross correlation (MCCC) method [11] requires prior knowledge of the RM positions and, more importantly, relies on the limiting assumption of a single-talker environment, i.e., no competing talkers are present.

The requirement of a single-talker environment or knowing the target talker in a multi-talker environment limits the use of existing methods [13], [14], [15], [16], [17], [18], [19], [20], [21], [22], for HA applications. In fact, HA users are commonly surrounded by multiple talkers, e.g., in restaurants, offices, and public transport. In such situations, the remote CS algorithm must first identify the target talker among the set of competing talkers, which is the problem addressed in this paper.

The problem of identifying the target talker in a multi-talker environment in a HA application is essentially ill-posed: it is very hard to identify the target talker without additional information about the target talker, e.g., physical location, signal characteristics, or the HA user's intention. The problem has previously been addressed using the *turn-taking* behavior of humans [26], [27], using *auditory attention decoding* [28], [29], [30], or simply via using a manual interface. *Turn-taking* based methods detect the target talker using speech gaps and overlaps in the conversation between the HA user and multiple candidate talkers in the acoustic scene, but they require robust VADs of candidate talkers and that the user is engaged in active conversation rather than just listening [31], [32]. Methods based on *auditory attention decoding* use electroencephalogram (EEG) or electrooculogram (EOG) electrodes to detect the HA users' attention or to monitor the HA user's eye-gaze to detect the target talker. Although various methods have been proposed that use EEG to detect the HA user's attention, the methods rely largely on the availability of wet EEG measurements recorded using bulky scalp electrodes [29]. Although methods using miniature electrodes in/ around the ear, the so-called ear-EEG [33], [34], increase their wearability factor, the development of wearable, robust EEG based HAs still remains a challenge. Lastly, selecting the target talker via a manual interface is less practical, particularly in dynamic acoustic situations.

Motivated by the recent development of wireless microphone accessories for HAs such as, clip-on microphones, e.g., [35], [36], and table microphones, e.g., [37], that are designed for HA users in challenging situations, e.g., social gatherings, our work focuses on CS in multi-talker situations, where the HA users have access to such RM accessories.

People, including HA users, use lip-reading to improve speech intelligibility and lower speech reception thresholds (SRTs) [38], [39], [40]. Moreover, HA users are recommended by hearing care professionals to lip read in social situations [41], [42], [43]. Therefore, HA users tend to, often, steer their heads toward their conversational partners in social settings. This fact has formed the basis for the frontal target talker assumptions in multi-microphone speech enhancement methods for HA applications [2].

In this paper, we use the head-steering direction of the HA user to address the problem of remote CS from a distributed

network of RM channels, in a dynamic, multi-talker environment, where in addition to the target talker, multiple competing talkers are present, without additional prior knowledge about the target talker location, signal characteristics or using additional sensors. We pose the CS task as a classification problem and derive an analytical solution using a multiple hypothesis test framework. We verify experimentally that the proposed method selects the remote channel that captures the target talker located along the head-steering direction, and consequently, selects the channel with the highest SNR. The results indicate that the proposed method outperforms state-of-the-art methods, in accurately identifying the remote channel. Moreover, we also demonstrate that the performance of the proposed method is robust to mismatches in the frontal relative acoustic transfer functions (RATFs) and analyze the performance of the proposed methods for non-frontal target talkers. Lastly, we illustrate a practical application of the proposed method in a conference room setting, where table microphone arrays are equipped with beamformers steered towards fixed locations. We show that the proposed method can accurately select the output of a table microphone beamformer that enhances the target talker, located in the head-steering direction of the HA user.

To limit the scope of this work, we consider the situation where multiple RM channels are transmitted to the HA as the fusion center. Challenges related to the transmission of multiple wireless channels to the HA such as, limited transmission power, bit-rate allocation, sample rate mismatch in the devices, are outside the scope of this study and we direct the reader to existing studies for more detailed discussions: [20], [44], [45]. Furthermore, in deriving the proposed method, we assume that the HA user steers their head in the direction of the target talker. In a real world situation, this may not constantly be the case, e.g., due to head movements of the user. However, such movements can relatively easily be devised, but is outside the scope of the paper. Besides, as we show in Section IV-A5, the proposed method is relatively insensitive to this assumption.

The structure of the paper is as follows. In Section II we present the signal model and notations that will be used in deriving the proposed method. In Section III, we derive analytical expressions for the proposed CS method. In Section IV, we analyze the performance of the proposed method through simulations and demonstrate practical applications. Lastly, we summarize and conclude our work in Section V.

## II. SIGNAL MODEL & NOTATIONS

Consider an acoustic setup, with a HA user wearing HAs, with  $M \geq 2$  microphones, surrounded by  $N + 1$  candidate talkers, see Figure 1. Let  $T_1$  be the target talker, while the candidate talkers,  $T_i$ ,  $i \geq 2$ , are the  $N$  competing talkers. Let there be remote acoustic sensors distributed around the acoustic scene that capture and transmit audio signals to the HA device. The remote acoustic sensors could be single RMs or microphone arrays, and the signals sent to the HA could be unprocessed or processed signals from each sensor. For simplicity, and without loss of generality, in this section, we assume the remote sensors to be RMs. The RMs can either be close-talking RMs located near the candidate talkers, e.g.,

clip-on microphones, or located elsewhere in the room, see Figure 1.

The short-time Fourier transform (STFT) coefficient vector of the noisy signal captured by the HA microphones,  $\mathbf{y}_{\text{HA}}(l, k) \in \mathbb{C}^{M \times 1}$ , is given by

$$\mathbf{y}_{\text{HA}}(l, k) = \mathbf{a}(\theta_1, k)S_1(l, k) + \underbrace{\sum_{i=2}^{N+1} \mathbf{a}(\theta_i, k)S_i(l, k) + \mathbf{v}_b(l, k)}_{\mathbf{v}_{\text{HA}}(l, k)}, \quad (1)$$

where,  $S_i(l, k) \in \mathbb{C}$  is the STFT coefficient of the speech signal from candidate talker  $T_i$ ,  $\mathbf{a}(\theta_i, k) \in \mathbb{C}^{M \times 1}$  is the head-related acoustic transfer function (ATF) vector from the  $i^{\text{th}}$  candidate talker to all  $M$  HA microphones,  $\mathbf{v}_b(l, k) \in \mathbb{C}^{M \times 1}$  is the STFT coefficient vector of the background noise component at the HA microphones, and  $\mathbf{v}_{\text{HA}}(l, k) \in \mathbb{C}^{M \times 1}$  is the STFT coefficient vector of the total noise component at the HA microphones, defined as the sum of the competing talkers and the background noise. Let  $\mathbf{d}(\theta_i, k) \in \mathbb{C}^{M \times 1}$ , be the RATF from

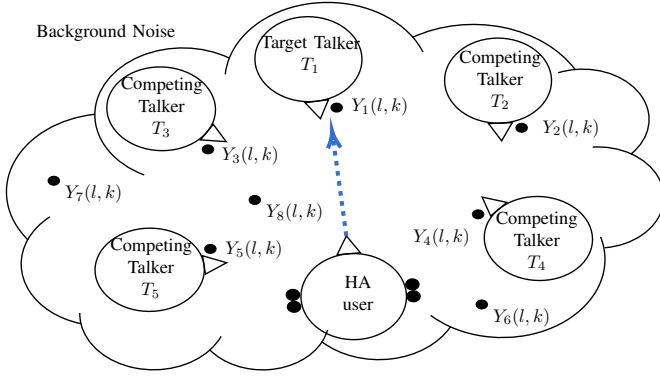


Fig. 1. Example acoustic scene with a HA user, with  $M \geq 2$  microphones, and with  $N + 1$  candidate talkers, with  $R$  RMs channels distributed around the scene. The HA user's head is steered towards the target talker,  $T_1$ . All the microphones are denoted by  $\bullet$ .

the  $i^{\text{th}}$  candidate talker to the HA microphones, measured w.r.t. an arbitrarily chosen HA reference microphone, i.e.,  $\mathbf{d}(\theta_i, k) = \frac{\mathbf{a}(\theta_i, k)}{A_{\text{ref}}(\theta_i, k)}$  [46], where  $A_{\text{ref}}(\theta_i, k) \in \mathbb{C}$ , is the ATF from the  $i^{\text{th}}$  candidate talker to the HA reference microphone. We can then rewrite (1) as

$$\mathbf{y}_{\text{HA}}(l, k) = \mathbf{d}(\theta_1, k)S_{1,\text{ref}}(l, k) + \mathbf{v}_{\text{HA}}(l, k), \quad (2)$$

where  $S_{1,\text{ref}}(l, k) \in \mathbb{C}$  is the STFT coefficient of the target speech signal at the HA reference microphone. We model the HA noise signal vector,  $\mathbf{v}_{\text{HA}}(l, k)$  as a zero-mean, complex Gaussian distributed random vector with a cross power spectral density matrix (CPSDM),  $\underline{\mathbf{C}}_{\text{v}}(l, k)$ , defined as

$$\underline{\mathbf{C}}_{\text{v}}(l, k) \triangleq \mathbb{E} [\mathbf{v}_{\text{HA}}(l, k) \mathbf{v}_{\text{HA}}^H(l, k)] \in \mathbb{C}^{M \times M}, \quad (3)$$

and the HA noisy CPSDM is defined as

$$\underline{\mathbf{C}}_{\text{y}}(l, k) \triangleq \mathbb{E} [\mathbf{y}_{\text{HA}}(l, k) \mathbf{y}_{\text{HA}}^H(l, k)] \in \mathbb{C}^{M \times M}. \quad (4)$$

Let there be  $R$  RMs placed in the acoustic scene. The STFT coefficient of the  $r^{\text{th}}$  noisy RM signal,  $Y_r(l, k) \in \mathbb{C}$ , is given by

$$Y_r(l, k) = A'_{1,r}(k)S_1(l, k) + \underbrace{\sum_{i=2}^{N+1} A'_{i,r}(k)S_i(l, k) + V_{b,r}(l, k)}_{V_r(l, k)}, \quad r=1, \dots, R, \quad (5)$$

where  $A'_{i,r}(k, l) \in \mathbb{C}$  is the ATF from the  $i^{\text{th}}$  candidate talker to the  $r^{\text{th}}$  RM,  $V_{b,r}(l, k)$  is the STFT coefficient of the background noise component at every  $r^{\text{th}}$  RM and  $V_r(l, k)$  is the STFT coefficient of the total noise component at the  $r^{\text{th}}$  RM, where the noise is the sum of the competing talkers and the background noise.

### III. PROPOSED METHOD

#### A. Problem formulation and Solution

We pose the task of CS based on the head-steering direction of the HA user, as a problem of classifying which  $r^{\text{th}}$  channel contains the target talker signal, and fits the signal model of the HA microphone signal. Specifically, we formulate the following multiple hypothesis testing problem

$$\mathcal{H}_r(l, k) : \mathbf{y}_{\text{HA}}(l, k) = \mathbf{d}(0^\circ, k)A_{1,r}(k)Y_r(l, k) + \mathbf{v}_{\text{HA}}(l, k), \quad r = 1, \dots, R, \quad (6)$$

where  $\mathcal{H}_r(l, k)$  denotes the hypothesis that the  $r^{\text{th}}$  channel contains the target talker signal,  $\mathbf{d}(0^\circ, k)$ , is the RATF from the frontal target talker, measured at the HA microphones relative to the HA reference microphone,  $A_{1,r}(k) \triangleq \frac{A_{\text{ref}}(k)}{A'_{1,r}(k)}$  is the RATF of the target talker, measured at the HA reference microphone, relative to the  $r^{\text{th}}$  RM. We assume all the ATFs to be shorter than the frame length of the STFT. Unlike in many existing speech enhancement schemes which require short STFT frames to limit the algorithm delay [46], [2], we can use longer frame-lengths here, as the proposed method is only used for remote CS.

In (6), by using a front-fixed RATF,  $\mathbf{d}(0^\circ, k)$ , we model the assumption that the HA user's head is steered towards the target talker. For the sake of clarity, let us briefly consider a constrained situation where the RMs in Figure 1 are close-talking RMs, such that the RMs capture only the clean signals from the candidate talkers,  $T_i$ , for  $1 \leq i \leq 5$ , such that  $Y_i(l, k) = A'_{i,i}(k)S_i(l, k)$  in (5). Then,  $Y_1(l, k)$ , captured by the RM placed on the target talker would perfectly fit the model in (6). Returning to the acoustic scene in Figure 1, when the RMs may be moved away from the candidate talkers, in addition to the target talker signal, the RMs would capture the competing talker signals and background noise, as in (5). This reduces the classification hypothesis in (6), to finding the RM closest to the target talker, who is located in the head-steering direction of the HA user.

Assuming equal prior probabilities of each hypothesis,  $\mathcal{H}_r(l, k)$ , the problem of minimising the probability of error of classification becomes a maximum likelihood problem [47]. Therefore, we select the  $r^{\text{th}}$  hypothesis,  $\mathcal{H}_r(l, k)$ , with

the highest conditional likelihood  $p(\mathbf{y}_{\text{HA}}(l, k) | \mathcal{H}_r)$ , and the channel selected is given by

$$\hat{r}_{\text{prop}}(l, k) = \underset{r \in \{1, \dots, R\}}{\operatorname{argmax}} p(\mathbf{y}_{\text{HA}}(l, k) | \mathcal{H}_r(l, k)). \quad (7)$$

In (6),  $\mathbf{d}(0^\circ, k)$ ,  $Y_r(l, k)$  are known, deterministic variables,  $\mathbf{v}_{\text{HA}}(l, k)$  is assumed to be zero-mean complex Gaussian distributed random vector with a CPSDM,  $\underline{\mathbf{C}}_{\text{v}}(l, k) \in \mathbb{C}^{M \times M}$ , so that  $\mathbf{y}_{\text{HA}}(l, k)$  is a non-zero mean, complex Gaussian distributed random vector. The conditional likelihood function,  $p(\mathbf{y}_{\text{HA}}(l, k) | \mathcal{H}_r(l, k))$ , parameterized by  $\phi_r(l, k) = \{Y_r(l, k), \mathbf{d}(0^\circ, k), \underline{\mathbf{C}}_{\text{v}}(l, k), A_{1,r}(k)\}$ , is then given by

$$\begin{aligned} p(\mathbf{y}_{\text{HA}}(l, k) | \mathcal{H}_r(l, k), \phi_r(l, k)) &= \frac{1}{\pi^M \det[\underline{\mathbf{C}}_{\text{v}}(l, k)]} \\ &\times \exp\left(-[\mathbf{y}_{\text{HA}}(l, k) - \mathbf{d}(0^\circ, k)\mu_r(l, k)]^H \right. \\ &\quad \times \underline{\mathbf{C}}_{\text{v}}^{-1}(l, k) \\ &\quad \left. \times [\mathbf{y}_{\text{HA}}(l, k) - \mathbf{d}(0^\circ, k)\mu_r(l, k)]\right), \end{aligned} \quad (8)$$

where  $\mu_r(l, k) \triangleq A_{1,r}(k)Y_r(l, k)$ .

Let the HA noisy signal data matrix of  $D$  noisy HA observations for a given frequency bin,  $k$ , be given by

$$\bar{\mathbf{y}}_{\text{HA}}(l, k) = [\mathbf{y}_{\text{HA}}(j_l, k) \quad \dots \quad \mathbf{y}_{\text{HA}}(j_u, k)], \quad (9)$$

where  $j_l = l - D + 1$  and  $j_u = l$ , and let the noisy data matrix, for all  $K$  frequency bins be

$$\bar{\bar{\mathbf{y}}}_{\text{HA}}(l) = [\bar{\mathbf{y}}_{\text{HA}}(l, 1) \quad \dots \quad \bar{\mathbf{y}}_{\text{HA}}(l, K)]. \quad (10)$$

Assuming that the STFT observations are independent across time-frame,  $l$  and frequency-bins,  $k$ , the joint conditional likelihood function is given by

$$\begin{aligned} p(\bar{\bar{\mathbf{y}}}_{\text{HA}}(l) | \mathcal{H}_r(l, k), \phi_r(l, k)) \\ = \prod_{k=1}^K \prod_{j=j_l}^{j_u} p(\mathbf{y}_{\text{HA}}(j, k) | \mathcal{H}_r(j, k), \phi_r(j, k)). \end{aligned} \quad (11)$$

Using the natural logarithm on both sides of (11), we get

$$\begin{aligned} \ln[p(\bar{\bar{\mathbf{y}}}_{\text{HA}}(l) | \mathcal{H}_r(l, k), \phi_r(l, k))] \\ = \sum_{k=1}^K \sum_{j=j_l}^{j_u} \ln p(\mathbf{y}_{\text{HA}}(j, k) | \mathcal{H}_r(j, k), \phi_r(j, k)) \\ = -KDM \ln \pi - \sum_{k=1}^K \sum_{j=j_l}^{j_u} \ln(\det[\underline{\mathbf{C}}_{\text{v}}(j, k)]) \\ - \sum_{k=1}^K \sum_{j=j_l}^{j_u} \mathbf{y}_{\text{HA}}^H(j, k) \underline{\mathbf{C}}_{\text{v}}^{-1}(j, k) \mathbf{y}_{\text{HA}}(j, k) \\ + \sum_{k=1}^K \sum_{j=j_l}^{j_u} [\mathbf{y}_{\text{HA}}^H(j, k) \underline{\mathbf{C}}_{\text{v}}^{-1}(j, k) \mathbf{d}(0^\circ, k) \mu_r(j, k) \\ + \mu_r^*(j, k) \mathbf{d}^H(0^\circ, k) \underline{\mathbf{C}}_{\text{v}}^{-1}(j, k) \mathbf{y}_{\text{HA}}(j, k) \\ - \mu_r^*(j, k) \mathbf{d}^H(0^\circ, k) \underline{\mathbf{C}}_{\text{v}}^{-1}(j, k) \mathbf{d}(0^\circ, k) \mu_r(j, k)]. \end{aligned} \quad (12)$$

Defining  $Y_{\text{mvdr}}(j, k) \triangleq \frac{\mathbf{d}^H(0^\circ, k) \underline{\mathbf{C}}_{\text{v}}^{-1}(j, k) \mathbf{y}_{\text{HA}}(j, k)}{\mathbf{d}^H(0^\circ, k) \underline{\mathbf{C}}_{\text{v}}^{-1}(j, k) \mathbf{d}(0^\circ, k)}$ , as the output of the HA minimum variance distortion-less response

(MVDR) beamformer, steered towards the front, and noting that the output noise power spectral density (PSD) of the MVDR beamformer is equal to  $\sigma_{\text{v,mvdr}}^2(l, k) = \frac{1}{\mathbf{d}^H(0^\circ, k) \underline{\mathbf{C}}_{\text{v}}^{-1}(l, k) \mathbf{d}(0^\circ, k)}$ , and that the first three terms in (12) are constant with respect to  $r$ , we can rewrite (12) as

$$\begin{aligned} \ln p(\bar{\bar{\mathbf{y}}}_{\text{HA}}(l) | \mathcal{H}_r(l, k), \phi_r(l, k)) \\ \propto \sum_{k=1}^K \left[ A_{1,r}(k) \sum_{j=j_l}^{j_u} \frac{Y_{\text{mvdr}}^*(j, k) Y_r(j, k)}{\sigma_{\text{v,mvdr}}^2(j, k)} \right. \\ \left. + A_{1,r}^*(k) \sum_{j=j_l}^{j_u} \frac{Y_r^*(j, k) Y_{\text{mvdr}}(j, k)}{\sigma_{\text{v,mvdr}}^2(j, k)} \right. \\ \left. - |A_{1,r}(k)|^2 \sum_{j=j_l}^{j_u} \frac{|Y_r(j, k)|^2}{\sigma_{\text{v,mvdr}}^2(j, k)} \right]. \end{aligned} \quad (13)$$

By maximizing (13) with respect to  $A_{1,r}(k)$ , we can find the maximum likelihood estimate of  $A_{1,r}(k)$  as

$$\hat{A}_{1,r}(k) = \frac{\sum_{j=j_l}^{j_u} \frac{Y_r^*(j, k) Y_{\text{mvdr}}(j, k)}{\sigma_{\text{v,mvdr}}^2(j, k)}}{\sum_{j=j_l}^{j_u} \frac{|Y_r(j, k)|^2}{\sigma_{\text{v,mvdr}}^2(j, k)}}. \quad (14)$$

Substituting the maximum likelihood estimate of  $A_{1,r}(k)$  from (14) in (13), the concentrated joint conditional log-likelihood function becomes

$$\begin{aligned} \ln p(\bar{\bar{\mathbf{y}}}_{\text{HA}}(l) | \mathcal{H}_r(l, k), \phi_r(l, k)) \\ \propto \sum_{k=1}^K \frac{\left| \sum_{j=j_l}^{j_u} \frac{Y_r^*(j, k) Y_{\text{mvdr}}(j, k)}{\sigma_{\text{v,mvdr}}^2(j, k)} \right|^2}{\sum_{j=j_l}^{j_u} \frac{|Y_r(j, k)|^2}{\sigma_{\text{v,mvdr}}^2(j, k)}}. \end{aligned} \quad (15)$$

We evaluate (15) for  $r = 1, \dots, R$ , to solve (7).

## B. Interpretation

To easily interpret the solution of the proposed method in (15), we introduce a few, additional assumptions here, which are not required to implement the proposed method in (15). Let the squared absolute correlation coefficient between the output signal of the head-steered MVDR beamformer,  $Y_{\text{mvdr}}(j, k)$ , and the  $r^{\text{th}}$  noisy RM signal,  $Y_r(j, k)$ , across  $D$  observations, be defined as

$$|\rho_r(l, k)|^2 \triangleq \frac{\left| \sum_{j=j_l}^{j_u} Y_r^*(j, k) Y_{\text{mvdr}}(j, k) \right|^2}{\sum_{j=j_l}^{j_u} |Y_r(j, k)|^2 \sum_{j=j_l}^{j_u} |Y_{\text{mvdr}}(j, k)|^2}, \quad (16)$$

where  $0 \leq |\rho_r(l, k)|^2 \leq 1$ . Let  $\hat{\sigma}_{\text{v,mvdr}}^2(l, k) = \sum_{j=j_l}^{j_u} \frac{|Y_{\text{mvdr}}(j, k)|^2}{D}$ , denote the estimate of the output noisy PSD of the MVDR beamformer. Assuming the output noise and the noisy PSDs of the MVDR beamformer to be constant across the  $D$  observations, and using (16) in (15), we can rewrite (7) as

$$\hat{r}_{\text{prop}}(l) = \underset{r \in \{1, \dots, R\}}{\text{argmax}} \sum_{k=1}^K \frac{\hat{\sigma}_{y, \text{mvdr}}^2(l, k)}{\sigma_{v, \text{mvdr}}^2(l, k)} |\rho_r(l, k)|^2. \quad (17)$$

From (17), it is clear that the proposed CS method selects the RM channel, which leads to the highest weighted squared absolute correlation coefficient between the output signal of the head-steered MVDR beamformer,  $Y_{\text{mvdr}}(l, k)$ , and the  $r^{\text{th}}$  RM signal,  $Y_r(l, k)$ . Note that the weighting across the  $k$  frequency bins is equal to the estimated posterior SNR of the HA MVDR beamformer,  $\hat{\gamma}_r(l, k) \triangleq \frac{\hat{\sigma}_{y, \text{mvdr}}^2(l, k)}{\sigma_{v, \text{mvdr}}^2(l, k)}$ . When the output SNR of the HA MVDR beamformer is low,  $\hat{\gamma}_r(l, k)$  tends to 1, and when it is high,  $\gamma_r(l, k)$  is greater than 1.

### C. Implementation

To implement the MVDR beamformer in (15), we require an estimate of the HA noise CPSDM,  $\underline{\mathbf{C}}_v(l, k)$ , which typically, would require a reliable VAD corresponding to the target talker [48]. In low SNR situations, with multiple competing talkers, such a target VAD is hard to realize. To circumvent this challenge, and due to the equivalence of the MVDR to the minimum power distortion-less response (MPDR) beamformer [49], we use the output of the MPDR beamformer,  $Y_{\text{mpdr}}(j, k) \triangleq \frac{\mathbf{d}^H(0^\circ, k) \underline{\mathbf{C}}_y^{-1}(j, k) \mathbf{y}_{\text{HA}}(j, k)}{\mathbf{d}^H(0^\circ, k) \underline{\mathbf{C}}_y^{-1}(j, k) \mathbf{d}(0^\circ, k)}$ , in (15) as it only requires the noisy CPSDM of the HA signals,  $\underline{\mathbf{C}}_y(l, k)$ . In acoustic beamformer applications, the MVDR beamformer is often preferred over the MPDR beamformer, as the latter tends to introduce audible distortions if the RATF,  $\mathbf{d}(0^\circ, k)$  is not estimated accurately. However, for our purposes, the output of the MPDR beamformer is not for listening, but for choosing the correct RM, which makes the use of the MPDR beamformer preferable in this situation. Furthermore, the solution in (15) requires the noise and noisy output PSDs of the MVDR beamformer,  $\sigma_{v, \text{mvdr}}^2(l, k)$ ,  $\hat{\sigma}_{y, \text{mvdr}}^2(l, k)$ , respectively, which are equal to the corresponding output PSDs of the MPDR beamformer,  $\sigma_{v, \text{mpdr}}^2(l, k)$ ,  $\hat{\sigma}_{y, \text{mpdr}}^2(l, k)$  [49]. As above, to estimate the noise PSD of the MPDR beamformer,  $\sigma_{v, \text{mpdr}}^2(l, k)$ , requires a good target talker VAD, which is hard to realize in the presence of multiple competing talkers. Therefore, for implementation purposes, we use  $\sigma_{v, \text{mpdr}}^2(l, k) = \hat{\sigma}_{y, \text{mpdr}}^2(l, k)$ , such that every frequency bin in (17) is weighted equally. Note that this approximation is reasonable for low SNRs. Furthermore, as we demonstrate in Section IV-A3, using  $\hat{\sigma}_{y, \text{mpdr}}^2(l, k)$  in place of  $\sigma_{v, \text{mpdr}}^2(l, k)$ , leads to very similar CS performance for realistic SNR in acoustic scenes.

We demonstrate the proposed CS method using close-talking RMs and table microphone arrays in Section IV. The signals used in the simulations are sampled at a sampling frequency of  $f_s = 16$  kHz and processed in the STFT domain, using 32 ms square-root Hann analysis and synthesis windows, with 50% overlap and FFT size of  $N_{\text{FFT}} = 512$  samples. This window length is chosen to ensure that it is longer than the effective duration of all acoustic impulse responses from source to microphones used. As the output of the beamformer is used only for the CS, which is not a time critical operation (15),

the use of longer analysis frames for STFT processing is permitted in the present context. This, consequently, increases the frequency resolution of processing and will accommodate longer acoustic impulse responses between the the different candidate talkers and the HA microphones, thereby eliminating the need for correlating across different time lags, as typically done when using shorter analysis frames. The duration of all signals used in the simulations is 30 s. The noisy CPSDM of the HA microphone signals,  $\underline{\mathbf{C}}_y(l, k)$  is estimated recursively at every frequency bin,  $k$ , as

$$\underline{\mathbf{C}}_y(l, k) = \alpha_y \underline{\mathbf{C}}_y(l-1, k) + (1 - \alpha_y) [\mathbf{y}_{\text{HA}}(l, k) \mathbf{y}_{\text{HA}}^H(l, k)], \quad (18)$$

where the smoothing co-efficient is  $\alpha_y = 0.8465$ , corresponding to a time-constant of 96 ms. We take the left-front HA microphone to be the HA reference microphone. For the simulations, we use only the left bilateral beamformer using the  $M = 4$  HA microphones, to implement the proposed method.

## IV. PERFORMANCE ANALYSIS

We analyze the performance of the proposed CS method in multi-talker scenarios, using close-talking RMs in Section IV-A and using table microphone arrays in Section IV-B.

### A. Simulation experiments using close-talking RMs

One of the common challenging situations for adults using HAs would be the dinner table settings, while for children using HAs it would be the classroom setting. Currently there are multiple wireless HA accessories like clip-on microphones or personal microphones that can be worn by the candidate talkers, and the signals are transmitted from a single or multiple RMs to the HA directly. Therefore, we evaluate the performance of the proposed CS method for the situation where each remote channel is captured by a RM, e.g., clip-on microphones.

1) *Simulation setup:* We simulate the acoustic scene shown in Figure 2, with a single HA user, wearing bilateral head-mounted HAs, i.e., HA units on both ears, in the presence of  $N+1$  candidate talkers, each wearing a RM, placed close to their mouths. The target talker is located in the head-steered direction of the HA user, i.e.,  $\theta_1 = 0^\circ$ , while the remaining  $N$  candidate talkers are competing talkers. We use speech signals from the English conversation dataset in [50], which consists of multiple two person conversation signals. We randomly assign the signals to all the candidate talkers. As shown in Figure 2, we place a RM close to each candidate talker, i.e.,  $R = N+1$  RMs, and every RM captures the target talker signal, but also the competing speech signals. In addition to the  $R$  RMs, we consider  $M = 4$  HA microphones of the bilateral HAs worn by the user, with  $\frac{M}{2} = 2$  microphones on each ear. We arbitrarily chose the left front microphone to be the HA reference microphone.

The HA microphone signals are simulated by convolving each candidate talker signal with the hearing aid head related impulse response (HAHRIR) from the respective candidate talker to the HA microphones, and by summing the convolved signals. Similarly, the RM signals are simulated by convolving the candidate talker signals with the RIR from each candidate

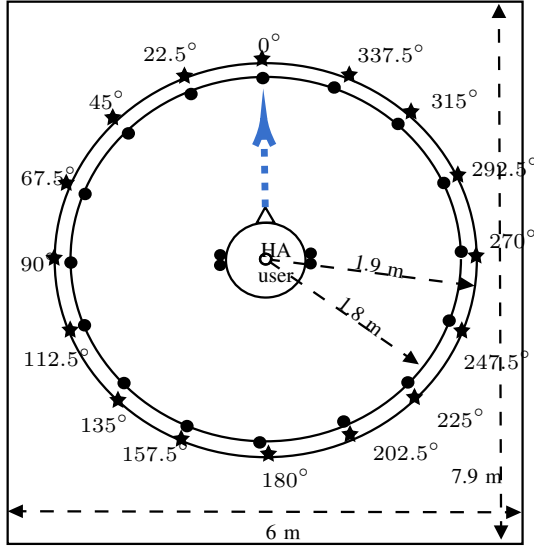


Fig. 2. Schematic diagram showing the source position ‘★’, and the chosen RM positions ‘●’, for the synthetic microphone RIR generated, based on the room characteristics in [51].

talker to the RMs in question, and summing the convolved signals. The HAHIRs, measured on a head-and-torso simulator (HATS) mannequin (*Subject 28*) in [51], are used to simulate the HA microphone signals, while the RIR with respect to the close-talking RMs are generated using the image method proposed in [52], using the room characteristics described in [51]. We simulate the HA user to be located at the center of the room and the candidate talkers to be located on a circle of radius 1.9 m, at 16 azimuthal angles, with the RMs located 0.2 m in front of the candidate talkers’ mouth, see Figure 2. We simulate the background noise at each HA microphone to be isotropic speech shaped noise (SSN) such that SNR of the target talker signal with respect to the background noise is 15 dB at the reference microphone, but note that the SNR reduces with every competing talker added to the scene. The isotropic SSN is generated by convolving SSN, whose spectral shape is determined from the long-term spectrum of the speech signals in [53], with the HAHIRs from the 16 azimuthal source positions to each HA microphone, and summing them at each microphone. We use independent SSN signals as the background noise at RMs, added at the same energy level as the isotropic SSN signal at the HA reference microphone. The frontal-RATF,  $d(0^\circ, k)$ , required in (12) is taken from [51].

The acoustic setup considered in Figure 2, there are 15 possible competing talker positions. In the following analysis we compare the CS performance by averaging the results across 40 combinations of uniformly randomly selected competing talker locations for  $N = \{2, \dots, 8\}$ , competing talkers. Furthermore, to assess the rapidity of the proposed method in adapting to the dynamics of the acoustic environment, we analyze the performance of CS as a function of the integration time,  $T_{\text{int}}$ , which corresponds to the number of  $D$  observations in (9), used to correlate the output signal of the MPDR,  $Y_{\text{mpdr}}(l, k)$  and the RM signals,  $Y_r(l, k)$  in (17).

In Figure 2, the target remote channel is the signal captured by the RM that is placed closest to the target talker located

in the head-steered direction of the HA user, i.e.,  $\theta_1 = 0^\circ$ . As mentioned previously, the SNR at the HA reference microphone and the RMs lowers with every competing talker added to the scene. Figure 3 shows the average input SNR at the HA reference microphone and the average input SNR at the RM placed on the target talker, across the number of competing talkers,  $N = \{2, \dots, 8\}$ , averaged across the 40 combinations of the competing talker positions, where the standard deviation is shown as error bar plots.

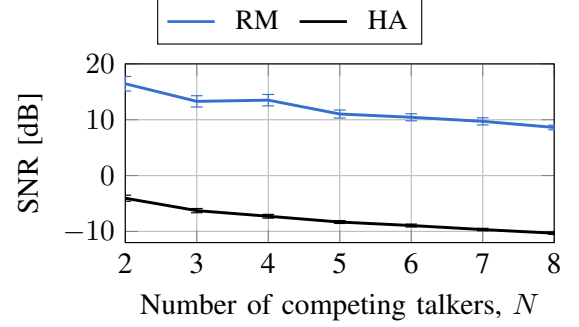


Fig. 3. Input SNR at the HA reference microphone and the RM placed on the target talker at  $\theta_1 = 0^\circ$ , across  $N = \{2, \dots, 8\}$ , number of competing talkers, for the acoustic scene in Figure 2.

2) *Baseline methods*: When each candidate talker is equipped with a RM, we can use the *turn-taking* behaviour [26], [27], between the HA user and the candidate talkers to find the target talker RM channel. For the acoustic scene described in Section IV-A1, we compare the performance of the proposed CS method, to the *turn-taking* based methods, normalized cross correlation (NCC) [31] and minimum overlap-gap (MOG) [32], in selecting the target talker channel.

a) *Normalized Cross-Correlation (NCC)* [31]: The NCC method identifies the target talker as the candidate talker whose binary voice activity sequence complements the HA user’s own-voice binary voice activity sequence. If  $V_0(l)$  denotes the HA user’s own-voice voice activity sequence, and  $V_r(l)$  denotes the voice activity sequence of the  $r^{\text{th}}$  candidate talker, at the  $l^{\text{th}}$  time-frame, the NCC decision can be written as [31]

$$\hat{r}_{\text{NCC}}(l) = \underset{r \in \{1, \dots, R\}}{\operatorname{argmax}} \frac{1 - \min_{p \in \{n_l, n_u\}} \mathcal{R}_{0,r}(p)}{2}, \quad (19)$$

where  $\mathcal{R}_{0,r}(p)$  is the cross-correlation, computed using an integration time,  $T_{\text{int}}$ , between the HA user’s own-voice voice activity sequence,  $V_0(l)$ , and the  $r^{\text{th}}$  candidate voice activity sequence,  $V_r(l)$ , at lag  $p$ .

b) *Minimum Overlap-Gap (MOG)* [32]: The MOG algorithm [32], identifies the target talker as the candidate talker, whose binary voice activity sequence,  $V_r(l)$ , maximizes the mean-square error (MSE) with respect to the HA user’s own-voice binary voice activity sequence,  $V_0(l)$  [32]:

$$\hat{r}_{\text{MOG}}(l) = \underset{r \in \{1, \dots, R\}}{\operatorname{argmax}} \mathbb{E} \left[ (V_0(l) - V_r(l))^2 \right], \quad (20)$$

computed using an integration time,  $T_{\text{int}}$ , at time-frame,  $l$ .



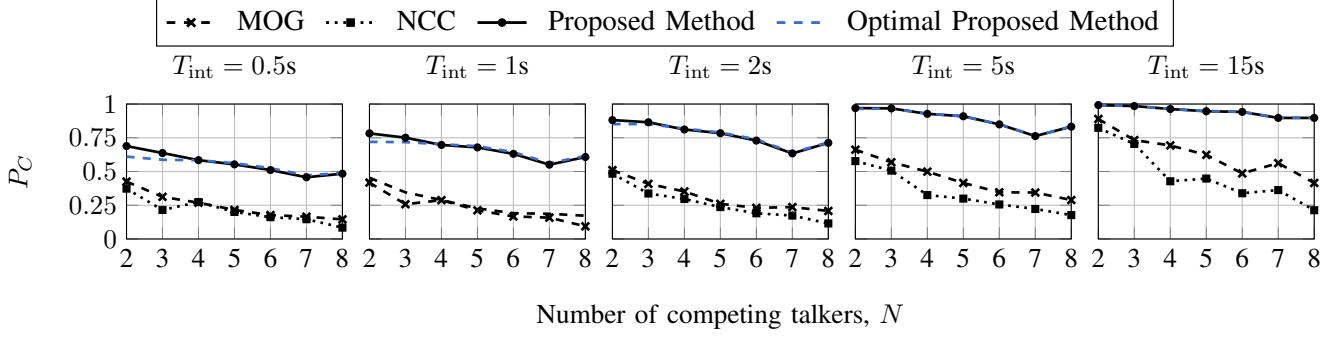


Fig. 4. Probability of correct target talker selection,  $P_C$ , using NCC, MOG and the Proposed Method, and Optimal Proposed Method, in the presence of  $N = \{2, 3, 4, 5, 6, 7, 8\}$  competing talkers, for  $T_{\text{int}} = \{0.5, 1, 2, 5, 15\}\text{s}$

3) *Results:* We compare the proposed CS method against NCC and MOG, in a multi-talker scenario. In our implementation of NCC and MOG, we use oracle VADs  $V_r(l, k)$ ,  $V_0(l, k)$ , estimated from the  $R$  clean candidate talker signals and HA user's own-voice signal, respectively. This gives NCC and MOG a very significant advantage over the proposed CS method.

In the following analysis, we introduce the probability of correct selection,  $P_C$ , of identifying the correct RM amongst the candidate RMs.  $P_C$  is defined as

$$P_C \triangleq \frac{\text{No. of time-frames the target RM is selected}}{\text{Total no. of time-frames}}. \quad (21)$$

Intuitively, when  $P_C = 1$ , it implies that the correct RM is chosen at all time-frames, while  $P_C = 1/R$  is a performance lower bound, which corresponds to the random selection of the target remote channel.

Figure 4 shows the performance of the proposed CS method, NCC and MOG in terms of  $P_C$ , as a function of number of competing talkers,  $N = \{2, \dots, 8\}$ , for different integration times,  $T_{\text{int}} = \{0.5, 1, 2, 5, 15\}\text{s}$ . As expected, the proposed method is more accurate for fewer competing talkers and longer integration times,  $T_{\text{int}}$ , because, with longer integration times,  $T_{\text{int}}$ , the correlation estimated between the output of the MPDR and the RM channel in (15) stabilizes. Note that since NCC and MOG rely on *turn-taking*, they require longer integration times,  $T_{\text{int}}$ , to identify the target talker accurately. From Figure 4, it is clear that the proposed method outperforms NCC and MOG in selecting the target talker RM, under all the number of competing talkers,  $N$ , and integration times,  $T_{\text{int}}$ , considered, despite MOG and NCC operating with ideal VADs.

To study the impact of the approximation,  $\sigma_{v, \text{mpdr}}^2(k, l) \approx \hat{\sigma}_{y, \text{mpdr}}^2(k, l)$ , that is used to implement the 'Proposed method', the 'Optimal Proposed method' curves in Figure 4 show the performance using  $\sigma_{v, \text{mpdr}}^2(k, l)$ , computed with access to noise components of the HA microphone signals in isolation, i.e., oracle information. As expected in Sec. III-C, at realistic SNRs used in the acoustic scene, see Figure 3, this approximation remains valid and the performance of the methods is very similar.

From Figure 4, it is evident that for all methods compared, performance increases with integration time,  $T_{\text{int}}$ . While the proposed CS method benefits from longer integration time

in order to correlate the output of the MPDR with the RM signals in (15), for the baseline *turn-taking* methods, longer integration time is useful to acquire more information regarding the speech gaps and overlaps during a conversation between the HA user and the candidate talkers. Nevertheless, the proposed CS method outperforms the baseline methods, even during shorter integration times.

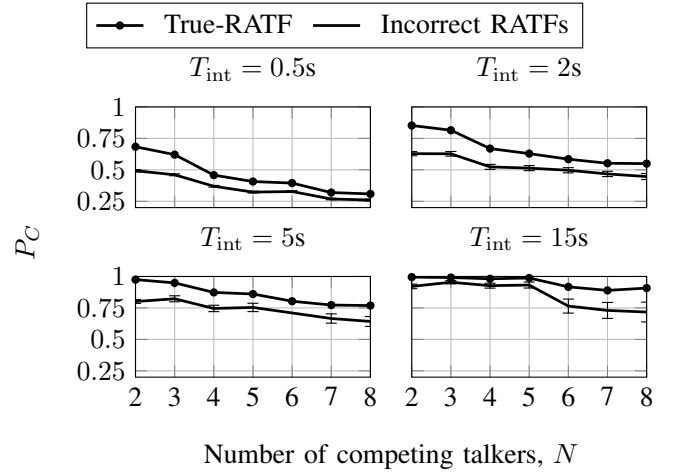


Fig. 5. Probability of correct target talker selection,  $P_C$ , using True-RATF, RATF vectors from different subjects in [51], in the presence of  $N = \{2, \dots, 8\}$  competing talkers, for  $T_{\text{int}} = \{0.5, 2, 5, 15\}\text{s}$ .

4) *Robustness to RATF mismatch:* The proposed CS method assumes that the target talker is located along the head-steering direction of the HA user and requires the frontal RATF vectors,  $\mathbf{d}(0^\circ, k)$ , in (12). In Section IV-A3, we used the RATF vectors, measured on the HATS mannequin, when simulating the acoustic scene. In reality, the frontal RATF would vary depending on the head size/shape of the HA user, head-and-torso acoustics and the position of the HAs. Nevertheless, the matched RATF situation simulated in Sec. IV-A3 could be achieved even in real-life situations using *in-situ* calibration methods [54] for estimating user-dependent individualized RATF vectors.

Even so, it is of interest to understand the robustness of the proposed CS method to incorrect frontal RATF vectors used. To do this, we test the proposed method using frontal RATF vectors measured on different heads, from [51], where

the authors measured the HAHIRs on 4 HATS mannequins, and 41 human subjects, using the same HA device. In this assessment, in addition to the frontal RATF vector used in Section IV-A1 (*Subject 28* in [51]), we use the frontal RATF from 20 randomly selected subjects. We compare the probability of correct selection,  $P_C$  (21), of the target RM located along the head-steering direction, when using ‘True-RATF’ (frontal RATF of *Subject 28*), and ‘Incorrect-RATFs’, (frontal RATFs from the 20 subjects).

Figure 5 shows the performance of the proposed CS method in terms of  $P_C$ , using the ‘True-RATF’ and the ‘Incorrect-RATFs’, across the number of competing talkers,  $N = \{2, \dots, 8\}$ , for integration times,  $T_{\text{int}} = \{0.5, 2, 5, 15\}$  s. The results from the 20 subjects of ‘Incorrect-RATFs’ are averaged and their standard deviations are shown as error bars. Clearly, using the ‘True-RATF’ results in better performance than using the ‘Incorrect-RATFs’. This is because, the spatial nulls introduced by the HA MPDR beamformer are less deep using the ‘Incorrect-RATFs’ than using the ‘True-RATF’. This results in lower noise reduction performance of the head-steered MPDR beamformer, which reduces,  $P_C$ . Nevertheless, when using higher integration times,  $T_{\text{int}}$ , the performance loss from using the ‘Incorrect-RATFs’ reduces. At lower integration times, the proposed CS method outperforms the baselines (see Figure 4), even with incorrect frontal RATFs used.

5) *Robustness to non-frontal target talker locations*: In dynamic acoustic situations, it is quite likely for the HA user to be moving their head to listen to multiple candidate talkers in the scene, and the HA user may therefore not perfectly steer their head towards the target talker at  $\theta_1 = 0^\circ$ , as assumed in (6). Alternatively, the target talker may not be located exactly in front of the HA user and the HA user’s head might occasionally be steered away from the target talker, while their eye gaze is steered towards the target talker. When the target talker location is non-frontal, i.e.,  $\theta_1 \neq 0^\circ$ , the assumption in (6) is violated, and therefore the performance is expected to be lower compared to when the assumption of frontal target talker, i.e.,  $\theta_1 = 0^\circ$  is met. In such cases, additional methods, e.g., *turn-taking* methods [31], [32], could be employed to enhance performance and improve overall results. Alternatively, or additionally, more advanced tracking methods might be employed which make better use of past values of the log-likelihood function in (15) by implicitly or explicitly taking into account the dynamics of head movements during conversations. Such methods are well outside the scope of this paper. However, for the purpose of a comprehensive analysis of the proposed CS method, this section presents the performance of the proposed CS method for non-frontal target talker locations.

To do so, for the acoustic scene in Sec. IV-A3, we test the proposed CS method using non-frontal target locations,  $\theta_1 = \{22.5^\circ, 337.5^\circ, 45^\circ, 315^\circ\}$ , while using a frontal RATF,  $\mathbf{d}(0^\circ, k)$ , from [51], in (12). We compare the performance of the proposed CS method for a frontal target talker,  $\theta_1 = 0^\circ$ , against non-frontal target talker locations,  $\theta_1 \neq 0^\circ$ . The performance is estimated in terms of probability of correct selection,  $P_C$  (21), of the target RM located closest to the target talker located at  $\theta_1$ .

Figure 6 shows the performance of the proposed CS

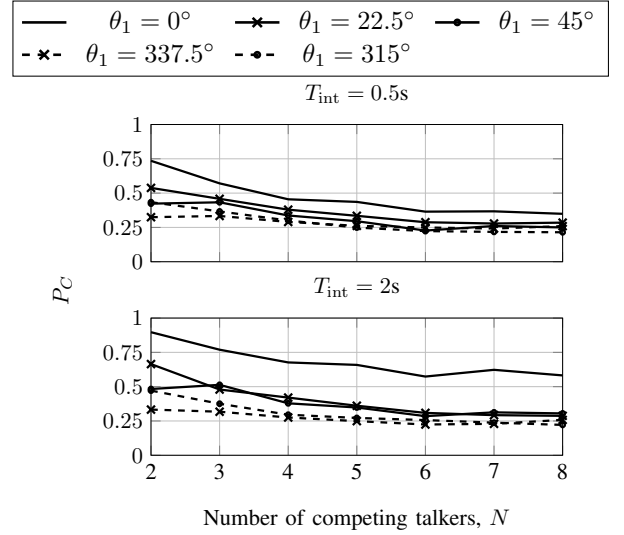


Fig. 6. Probability of correct target talker selection,  $P_C$ , using RATF vectors,  $\mathbf{d}(\theta, k)$  steered towards  $\theta = \{0^\circ, 22.5^\circ, 337.5^\circ, 45^\circ, 315^\circ\}$  in [51], in the presence of  $N = \{2, \dots, 8\}$  competing talkers, for  $T_{\text{int}} = \{0.5, 2\}$  s.

method in terms of  $P_C$ , for target talker locations,  $\theta_1 = \{0^\circ, 22.5^\circ, 337.5^\circ, 45^\circ, 315^\circ\}$ , across the number of competing talkers,  $N = \{2, 3, 4, 5, 6, 7, 8\}$ , for the integration times  $T_{\text{int}} = \{0.5, 2\}$  s. In the simulations, we ensure that a competing talker is not located along the head steering direction. The results shown are averaged over 40 combinations of the competing talker positions.

From Figure 6, it can be observed that the proposed CS method performs best when the HA user’s head is steered towards the direction of the target talker ( $\theta_1 = 0^\circ$ ), as assumed in (6). Moreover, as expected, the loss in probability of correct selection,  $P_C$ , increases with the angle mismatch. Note that, we use the left front microphone as the reference microphone for the HA MPDR. Due to the head shadow effect, the spatial response of the HA MPDR becomes asymmetric for target locations on the right of the HA user, i.e.,  $180^\circ < \theta_1 < 360^\circ$ , compared to targets located to the left, i.e.,  $0^\circ < \theta_1 < 180^\circ$ . Therefore, in Figure 6, we observe  $P_C$  to be lower for target locations on the right at  $\theta_1 = \{315^\circ, 337.5^\circ\}$  when compared to target locations on the left at  $\theta_1 = \{22.5^\circ, 45^\circ\}$ , even though they are symmetrically located w.r.t the HA user’s head. In such situations, the loss in performance could be diminished by combining the left-right HA channel selection decisions. Nevertheless, the performance of the proposed CS method even for non-frontal target talker locations exceeds the performance of the baseline methods discussed previously in Section IV-A3 (cf. Figure 4). Moreover, similar to the trend observed in Sec. IV-A3, in the presence of fewer competing talkers, e.g.,  $N < 4$ ,  $P_C$  increases with longer integration times,  $T_{\text{int}}$ .

### B. Simulation experiments using table microphone arrays

Since using individual RMs for each candidate talker is not always feasible, here we consider a situation where a table microphone is accessible to the HA user. In this situation, the table microphone separates the multiple candidate talkers in



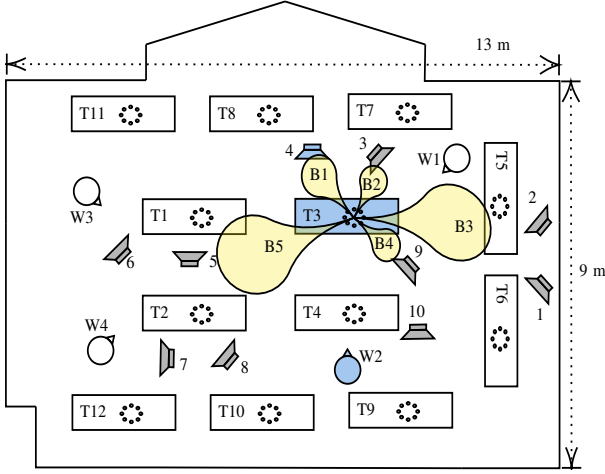


Fig. 7. Sketch showing the target talker position ‘4’, the table microphone array, ‘T3’, and the position of HA user, ‘W2’, as measured in [55]. Also, the MPDR beamformers, B1-B5, from the table microphone T3 are shown.

the scene, e.g., via beamforming or using speaker separation algorithms, among which the proposed CS method must select the target talker. In particular, we demonstrate that the proposed CS method accurately selects the channel containing the frontal target talker, when choosing among enhanced candidate talker signals from beams steered in different directions in the room.

1) *Simulation Setup:* To simulate the acoustic scene, we use HAHIRs and RIRs from [55], measured in a large, reverberant conference room ( $T_{60} = 800$  ms). The acoustic scene described in [55], is illustrated in Figure 7, where four HA users are denoted by W1-W4, 10 loudspeakers are denoted by numbers 1–10, that act as candidate sources. Multiple tables are placed in the room, with 12 table microphone arrays, denoted by T1-T12, each containing 8 microphones in a circular array. We use the HA user, W2, with  $M = 4$  microphones (front and rear microphones on both ears), the table microphone array, T3, with 8 microphones, the loudspeaker located at ‘4’, as the target talker and the remaining loudspeakers as competing talkers. The head-steered MPDR beamformer of the HA user, W2, is pointing frontal towards the target talker located at ‘4’. The table microphone, T3, has fixed MPDR beamformers directed towards candidate talkers:  $\{4, 3, 2, 9, 5\}$ , denoted by, B1-B5 (see Figure 7). The output of the table microphone MPDR beamformers represent the  $R$  remote channels, from which the proposed method must identify the channel that best corresponds to the signal from the frontal talker at ‘4’. Note that the table microphone beamformers are chosen to be MPDR beamformers for convenience, however, in reality can represent other speech enhancement algorithms.

The microphone signals at the HA, W2, are generated by convolving the candidate talker signals with HAHIR from the corresponding candidate talker to the HA microphones. Similarly, the signals at the table microphone array, T3, are generated by convolving the candidate talker signals with RIRs from the corresponding candidate talker to the RMs. We add the background noise recorded in [55]. We implement the MPDR beamformers at the table microphone, T3, steered towards the

candidate talkers:  $\{4, 3, 2, 9, 5\}$ , using the ATFs from [55]. For the target talker at ‘4’, the channel of interest is the output of MPDR beamformer, B1.

2) *Results:* Our goal is to identify how accurately the proposed method identifies the target RM (many speech enhancement systems can be envisaged from this, but they are beyond our scope). Hence, we quantify the performance of the proposed method using the probability of selection of the  $r^{\text{th}}$  channel,

$$P_{S_r} = \frac{\text{No. of time-frames } r^{\text{th}} \text{ channel is selected}}{\text{Total no. of time-frames}}, \quad (22)$$

where  $r \in \{1, \dots, R\}$ .

The first row of Figure 8 shows the output SNRs of the HA MPDR beamformer and the fixed MPDR beamformers, B1-B5, at the table microphones, T3, where the SNR is defined as the power of the target talker signal relative to the power of the noise signals in the output signal of the MPDR beamformer. There are 9 competing talker locations, and the output SNRs plotted are averaged across 20 combinations of uniformly randomly selected competing talker locations for  $N = \{3, \dots, 7\}$ , and the standard deviations are shown as error bars. From the SNR plots, we infer that it would be highly beneficial to be able to select the channel corresponding to the output of the MPDR beamformer, B1, as it has an SNR that is 3–6 dB higher than any other MPDR beamformer, including that of the HA MPDR beamformer, which serves as a natural baseline.

The second row of Figure 8 shows the results in terms of  $P_{S_r}$ , for competing talkers,  $N = \{3, \dots, 7\}$ , for different integration times,  $T_{\text{int}} = \{0.5, 1, 2\}$  s, across 20 combinations of competing talkers positions. As expected,  $P_{S_r}$  of the channel from B1, is high, i.e.,  $P_{S_r} \geq 0.9$  for B1 for all number of competing talkers,  $N$  and integration times,  $T_{\text{int}}$ .

## V. CONCLUSION

We consider the problem of channel selection (CS) for hearing aid (HA) applications using remote microphones (RMs), in acoustic situations with multiple competing talkers. We use the head-steering direction of the HA user to pose the CS problem in a multiple hypothesis test framework and derive a maximum likelihood solution. The proposed method chooses the RM channel that leads to the highest weighted squared absolute correlation coefficient between the output of the head-steered HA minimum variance distortionless response (MVDR) beamformer and the RM channel. Through simulations using realistic acoustic scenes using close-talking RMs and table microphone arrays, we show that the proposed CS method accurately selects the RM channel located in the head-steering direction of the HA user. Furthermore, we demonstrate that the proposed CS method, without the need for additional sensors, significantly outperforms its baselines in the presence of multiple competing talkers.

## REFERENCES

- [1] M. Brandstein and D. Ward, *Microphone arrays: signal processing techniques and applications*. Springer Science & Business Media, 2001.

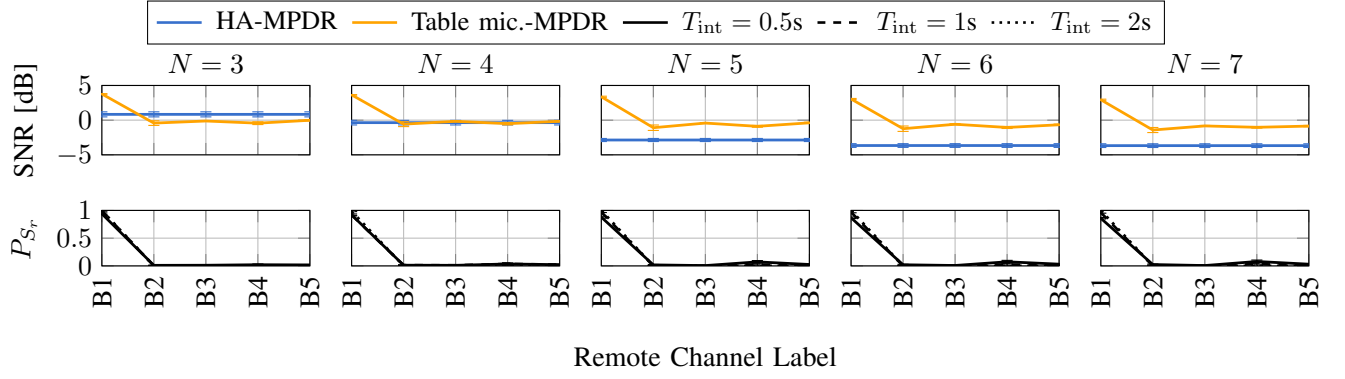


Fig. 8. Performance of the proposed CS method in terms of  $P_{S_r}$  for beams: {B1, B2, B3, B4, B5}, in the presence of  $N = \{3, 4, 5, 6, 7\}$ , using integration times,  $T_{\text{int}} = \{0.5, 1, 2\}$ s for table microphone arrays.

- [2] S. Doclo, W. Kellermann, S. Makino, and S. E. Nordholm, "Multichannel signal enhancement algorithms for assisted listening devices: Exploiting spatial diversity using multiple microphones," *IEEE Signal Processing Magazine*, vol. 32, no. 2, pp. 18–30, 2015.
- [3] A. Bertrand, "Applications and trends in wireless acoustic sensor networks: A signal processing perspective," in *Symposium on Communications and Vehicular Technology in the Benelux (SCVT)*. IEEE, 2011, pp. 1–6.
- [4] M. Wölfel and J. McDonough, *Distant speech recognition*. John Wiley & Sons, 2009.
- [5] L. Thibodeau, "Comparison of speech recognition with adaptive digital and fm remote microphone hearing assistance technology by listeners who use hearing aids," *American Journal of Audiology*, vol. 23, no. 2, pp. 201–210, 2014.
- [6] A. Boothroyd, "Hearing aid accessories for adults: The remote fm microphone," *Ear and Hearing*, vol. 25, no. 1, pp. 22–33, 2004.
- [7] L. M. Thibodeau, "Benefits in speech recognition in noise with remote wireless microphones in group settings," *Journal of the American Academy of Audiology*, vol. 31, no. 06, pp. 404–411, 2020.
- [8] G. De Ceulaer, J. Bestel, H. E. Müller, F. Goldbeck, S. P. J. de Varebeke, and P. J. Govaerts, "Speech understanding in noise with the Roger Pen, Naida CI Q70 processor, and integrated Roger 17 receiver in a multi-talker network," *European Archives of Oto-rhino-laryngology*, vol. 273, pp. 1107–1114, 2016.
- [9] J. M. Kates, K. H. Arehart, and L. O. Harvey, "Integrating a remote microphone with hearing-aid processing," *The Journal of the Acoustical Society of America*, vol. 145, no. 6, pp. 3551–3566, 2019.
- [10] N. Gößling, "Binaural beamforming algorithms and parameter estimation methods exploiting external microphones," Ph.D. thesis, Carl von Ossietzky Universität Oldenburg, 2020.
- [11] K. Kumatani, J. McDonough, J. F. Lehman, and B. Raj, "Channel selection based on multichannel cross-correlation coefficients for distant speech recognition," in *Joint Workshop on Hands-free Speech Communication and Microphone Arrays*. IEEE, 2011, pp. 1–6.
- [12] A. Bertrand and M. Moonen, "Robust distributed noise reduction in hearing aids with external acoustic sensor nodes," *EURASIP Journal on Advances in Signal Processing*, pp. 1–14, 2009.
- [13] —, "Efficient sensor subset selection and link failure response for linear MMSE signal estimation in wireless sensor networks," in *European Signal Processing Conference (EUSIPCO)*. IEEE, 2010, pp. 1092–1096.
- [14] A. Bertrand, J. Szurley, P. Ruckebusch, I. Moerman, and M. Moonen, "Efficient calculation of sensor utility and sensor removal in wireless sensor networks for adaptive signal estimation and beamforming," *IEEE Transactions on Signal Processing*, vol. 60, no. 11, pp. 5857–5869, 2012.
- [15] J. Szurley, A. Bertrand, and M. Moonen, "Efficient computation of microphone utility in a wireless acoustic sensor network with multi-channel Wiener filter based noise reduction," in *International Conference on Acoustics, Speech and Signal Processing (ICASSP)*. IEEE, 2012, pp. 2657–2660.
- [16] J. Szurley, A. Bertrand, M. Moonen, P. Ruckebusch, and I. Moerman, "Energy aware greedy subset selection for speech enhancement in wireless acoustic sensor networks," in *European Signal Processing Conference (EUSIPCO)*. IEEE, 2012, pp. 789–793.
- [17] J. Szurley, A. Bertrand, P. Ruckebusch, I. Moerman, and M. Moonen, "Greedy distributed node selection for node-specific signal estimation in wireless sensor networks," *Signal Processing*, vol. 94, pp. 57–73, 2014.
- [18] J. Zhang, S. P. Chepuri, R. C. Hendriks, and R. Heusdens, "Microphone subset selection for mvdr beamformer based noise reduction," *IEEE/ACM Transactions on Audio, Speech, and Language Processing*, vol. 26, no. 3, pp. 550–563, 2018.
- [19] J. Zhang, J. Du, and L.-R. Dai, "Sensor selection for relative acoustic transfer function steered linearly-constrained beamformers," *IEEE/ACM Transactions on Audio, Speech, and Language Processing*, vol. 29, pp. 1220–1232, 2021.
- [20] M. Gunther, H. Afifi, A. Brendel, H. Karl, and W. Kellermann, "Network-aware optimal microphone channel selection in wireless acoustic sensor networks," in *International Conference on Acoustics, Speech and Signal Processing (ICASSP)*. IEEE, 2021, pp. 820–824.
- [21] M. Günther, A. Brendel, and W. Kellermann, "Online estimation of time-variant microphone utility in wireless acoustic sensor networks using single-channel signal features," in *European Signal Processing Conference (EUSIPCO)*. IEEE, 2021, pp. 1120–1124.
- [22] —, "Microphone utility estimation in acoustic sensor networks using single-channel signal features," *EURASIP Journal on Audio, Speech, and Music Processing*, vol. 2023, no. 1, p. 29, 2023.
- [23] M. Wölfel, C. Fügen, S. Ikbāl, and J. W. McDonough, "Multi-source far-distance microphone selection and combination for automatic transcription of lectures," in *International Conference on Spoken Language Processing*, 2006.
- [24] M. Wolf and C. Nadeu, "Channel selection measures for multi-microphone speech recognition," *Speech Communication*, vol. 57, pp. 170–180, 2014.
- [25] I. Himawan, I. McCowan, and S. Sridharan, "Clustering of ad-hoc microphone arrays for robust blind beamforming," in *International Conference on Acoustics, Speech and Signal Processing (ICASSP)*. IEEE, 2010, pp. 2814–2817.
- [26] H. Sacks, E. A. Schegloff, and G. Jefferson, "A simplest systematics for the organization of turn taking for conversation," in *Studies in the organization of conversational interaction*. Elsevier, 1978, pp. 7–55.
- [27] I. McCowan, S. Bengio, D. Gatica-Perez, G. Lathoud, F. Monay, D. Moore, P. Wellner, and H. Bourlard, "Modeling human interaction in meetings," in *International Conference on Acoustics, Speech, and Signal Processing (ICASSP)*, vol. 4. IEEE, 2003, pp. IV–748.
- [28] E. Alickovic, T. Lunner, F. Gustafsson, and L. Ljung, "A tutorial on auditory attention identification methods," *Frontiers in neuroscience*, vol. 13, p. 153, 2019.
- [29] S. Geirnaert, S. Vandecappelle, E. Alickovic, A. De Cheveigne, E. Lalor, B. T. Meyer, S. Miran, T. Francart, and A. Bertrand, "Electroencephalography-based auditory attention decoding: Toward neurosteered hearing devices," *IEEE Signal Processing Magazine*, vol. 38, no. 4, pp. 89–102, 2021.
- [30] B. Mirkovic, M. G. Bleichner, M. De Vos, and S. Debener, "Target speaker detection with concealed eeg around the ear," *Frontiers in neuroscience*, vol. 10, p. 349, 2016.
- [31] A. Harma and K. Pham, "Conversation detection in ambient telephony," in *International Conference on Acoustics, Speech and Signal Processing (ICASSP)*. IEEE, 2009, pp. 4641–4644.
- [32] P. Hoang, Z.-H. Tan, J. M. De Haan, and J. Jensen, "The Minimum

- Overlap-Gap Algorithm for Speech Enhancement,” *IEEE Access*, vol. 10, pp. 14 698–14 716, 2022.
- [33] G. Ciccarelli, M. Nolan, J. Perricone, P. T. Calamia, S. Haro, J. O’Sullivan, N. Mesgarani, T. F. Quatieri, and C. J. Smalt, “Comparison of two-talker attention decoding from EEG with nonlinear neural networks and linear methods,” vol. 9, no. 1, p. 11538.
- [34] J. W. Kam, S. Griffin, A. Shen, S. Patel, H. Hinrichs, H.-J. Heinze, L. Y. Deouell, and R. T. Knight, “Systematic comparison between a wireless EEG system with dry electrodes and a wired EEG system with wet electrodes,” *NeuroImage*, vol. 184, pp. 119–129, 2019.
- [35] D. Gordey, “ConnectClip: A Guide to Better Communication,” Oticon A/S, White Paper, 2019.
- [36] Phonak, “Roger Pen: Bridging the understanding gap,” Phonak AG, White Paper, 2013.
- [37] —, “Roger™ Multibeam Technology - Enhancing the Group Listening Experience,” Phonak, White Paper, 2018.
- [38] M. Middelweerd and R. Plomp, “The effect of speechreading on the speech-reception threshold of sentences in noise,” *The Journal of the Acoustical Society of America*, vol. 82, no. 6, pp. 2145–2147, 1987.
- [39] N. P. Erber, “Interaction of audition and vision in the recognition of oral speech stimuli,” *Journal of speech and hearing research*, vol. 12, no. 2, pp. 423–425, 1969.
- [40] L. E. Bernstein, N. Jordan, E. T. Auer, and S. P. Eberhardt, “Lipreading: A review of its continuing importance for speech recognition with an acquired hearing loss and possibilities for effective training,” *American Journal of Audiology*, vol. 31, no. 2, pp. 453–469, 2022.
- [41] M. Valente, “Guideline for audiologic management of the adult patient,” *Audiology Online*, 2006.
- [42] S. S. Chandrasekhar, B. S. Tsai Do, S. R. Schwartz, L. J. Bontempo, E. A. Faucett, S. A. Finestone, D. B. Hollingsworth, D. M. Kelley, S. T. Kmucha, G. Moonis *et al.*, “Clinical practice guideline: sudden hearing loss (update),” *Otolaryngology–Head and Neck Surgery*, vol. 161, no. 1\_suppl, pp. S1–S45, 2019.
- [43] L. Turton, P. Souza, L. Thibodeau, L. Hickson, R. Gifford, J. Bird, M. Stropahl, L. Gailey, B. Fulton, N. Scarinci *et al.*, “Guidelines for best practice in the audiological management of adults with severe and profound hearing loss,” in *Seminars in hearing*, vol. 41, no. 03. Thieme Medical Publishers, Inc., 2020, pp. 141–246.
- [44] J. Zhang, R. Heusdens, and R. C. Hendriks, “Sensor selection and rate distribution based beamforming in wireless acoustic sensor networks,” in *European Signal Processing Conference (EUSIPCO)*. IEEE, 2019, pp. 1–5.
- [45] J. Zhang, R. Tao, J. Du, and L.-R. Dai, “Energy-efficient sparsity-driven speech enhancement in wireless acoustic sensor networks,” *IEEE/ACM Transactions on Audio, Speech, and Language Processing*, vol. 31, pp. 215–228, 2023.
- [46] S. Gannot, D. Burshtein, and E. Weinstein, “Signal enhancement using beamforming and nonstationarity with applications to speech,” *IEEE Transactions on Signal Processing*, vol. 49, no. 8, pp. 1614–1626, 2001.
- [47] S. M. Kay, *Fundamentals of statistical signal processing: Detection Theory*. Prentice-Hall, Inc., 1998.
- [48] C. Breithaupt and R. Martin, *Noise reduction-statistical analysis and control of musical noise*. New York, USA: Wiley, 2008.
- [49] H. L. Van Trees, *Optimum array processing: Part IV of detection, estimation, and modulation theory*. John Wiley & Sons, 2002.
- [50] A. J. Sørensen, M. Fereczkowski, and E. MacDonald, “Task dialog by native-danish talkers in danish and english in both quiet and noise,” *Zenodo*, vol. 10, 2018.
- [51] A. H. Moore, J. M. de Haan, M. S. Pedersen, P. A. Naylor, M. Brookes, and J. Jensen, “Personalized signal-independent beamforming for binaural hearing aids,” *The Journal of the Acoustical Society of America*, vol. 145, no. 5, pp. 2971–2981, 2019.
- [52] J. B. Allen and D. A. Berkley, “Image method for efficiently simulating small-room acoustics,” *The Journal of the Acoustical Society of America*, vol. 65, no. 4, pp. 943–950, 1979.
- [53] J. S. Garofolo, L. F. Lamel, W. M. Fisher, J. G. Fiscus, and D. S. Pallett, “DARPA TIMIT acoustic-phonetic continuous speech corpus CD-ROM. NIST speech disc 1-1.1,” vol. 93, 1993.
- [54] J. Jensen and M. S. Pedersen, “Self-calibration of multi-microphone noise reduction system for hearing assistance devices using an auxiliary device,” Mar. 7 2017, US Patent 9,591,411 B2.
- [55] R. Corey, M. Skarha, and A. Singer, “Massive distributed microphone array dataset,” *University of Illinois at Urbana-Champaign*, 2019.

## VI. BIOGRAPHY SECTION

**VASUDHA SATHYAPRIYAN** received the M.Sc. degree (cum laude) in Electrical Engineering from Delft University of Technology, Delft, The Netherlands in 2020. She is currently pursuing a Ph.D degree in Electrical Engineering from Aalborg University, in collaboration with Demant A/S, Denmark.

**MICHAEL S. PEDERSEN** received the M.S. degree from the Technical University of Denmark (DTU), Lyngby, Denmark, in 2003 and the Ph.D. degree from the Section for Intelligent Signal Processing, Department of Mathematical Modelling, DTU, in 2006. Since 2001, he has been with the hearing instrument company, Demant A/S, as a Principal Specialist. He has authored or coauthored more than 20 peer reviewed publications, and he is listed as an inventor on more than 60 patent applications.

**MIKE BROOKES** is an Emeritus Reader in Signal Processing in the Department of Electrical and Electronic Engineering at Imperial College London. After graduating in Mathematics from Cambridge University in 1972, he worked at the Massachusetts Institute of Technology before returning to the UK and joining Imperial College in 1977.

**JAN ØSTERGAARD** received the M.Sc.E.E. degree from Aalborg University, Aalborg, Denmark, in 1999 and the Ph.D. degree (cum laude) from the Delft University of Technology, Delft, The Netherlands, in 2007. He was an R&D Engineer with ETI Inc., Chantilly, VA, USA. Between September 2007 and June 2008, he was a Postdoctoral Researcher with The University of Newcastle, Callaghan, NSW, Australia. He is currently a Professor in information theory and signal processing, the Head of the Section on AI and Sound, and the Head of the Centre for Acoustic Signal Processing Research with Aalborg University.

**PATRICK A. NAYLOR** received the B.Eng. degree in electronic and electrical engineering from the University of Sheffield, Sheffield, U.K., and the Ph.D. degree from Imperial College London, London, U.K. He is currently a Professor of speech and acoustic signal processing with Imperial College London. His research interests include speech, audio and acoustic signal processing. His current research addresses microphone array signal processing, speaker diarization, and multichannel speech enhancement for application to binaural hearing aids and robot audition. He has also worked on speech dereverberation including blind multichannel system identification and equalization, acoustic echo control, non-intrusive speech quality estimation, and speech production modeling with a focus on the analysis of the voice source signal. In addition to his academic research, he enjoys several collaborative links with industry.

**JESPER JENSEN** received the M.Sc. degree in electrical engineering and the Ph.D. degree in signal processing from Aalborg University, Aalborg, Denmark, in 1996 and 2000, respectively. From 1996 to 2000, he was with Center for Person Kommunikation, Aalborg University, as a Ph.D. student and an Assistant Research Professor. From 2000 to 2007, he was a Postdoctoral Researcher and an Assistant Professor with the Delft University of Technology, Delft, The Netherlands, and an External Associate Professor with Aalborg University. He is currently a Fellow with Demant A/S, Smørum, Denmark, where his main responsibility is scouting and development of new signal processing concepts for hearing aid applications. He is a Professor with the Section for Signal and Information Processing, Department of Electronic Systems, Aalborg University. He is also a Co-Founder of Centre for Acoustic Signal Processing Research, Aalborg University. His main research interests include acoustic signal processing, including signal retrieval from noisy observations, coding, speech, and audio modification and synthesis, intelligibility enhancement of speech signals, signal processing for hearing aid applications, and perceptual aspects of signal processing.